

Another possibility is that the brain's enormous intrinsic functional activity facilitates responses to stimuli. Neurons continuously receive both excitatory and inhibitory inputs. The "balance" of these stimuli determines the responsiveness (or gain) of neurons to correlated inputs and, in so doing, potentially sculpts communication pathways in the brain (4). Balance also manifests at a large systems level. For example, neurologists know that strokes that damage cortical centers that control eye movements lead to deviation of the eyes toward the side of the lesion, implying the preexisting presence of "balance." It may be that in the normal brain, a balance of opposing forces enhances the precision of a wide range of processes. Thus, "balance" might be viewed as a necessary enabling, but costly, element of brain function.

A more expanded view is that intrinsic activity instantiates the maintenance of information for interpreting, responding to, and even predicting environmental demands. In this regard, a useful conceptual framework from theoretical neuroscience posits that the brain operates as a Bayesian inference engine, designed to generate predictions about the future (5). Beginning with a set of "advance" predictions at birth (genes), the brain is then sculpted by worldly experience to represent intrinsically a "best guess" ("priors" in Bayesian parlance) about the environment and, in the case of humans at least, to make predictions about the future (6). It has long been thought that the ability to reflect on the past or contemplate the future has facilitated the development of unique human attributes such as imagination and creativity (7, 8).

fMRI provides one important experimental approach to understanding the nature of the brain's intrinsic functional activity without direct recourse to controlled stimuli and observable behaviors. A prominent feature of fMRI is that the unaveraged signal is quite noisy, prompting researchers to average their data to reduce this "noise" and increase the signals they seek. In doing this, it turns out that a considerable fraction of the variance in the blood oxygen level-dependent (BOLD) signal of fMRI in the frequency range below 0.1 Hz, which reflects fluctuating neural activity, is lost. This activity exhibits striking patterns of coherence within known networks of specific neurons in the human brain in the absence of observable behaviors (see the figure).

Future research should address the cellular events underlying spontaneous fMRI BOLD signal fluctuations. Studies likely will cover a broad range of approaches to the study of spontaneous activity of neurons (9,

10). In this regard, descriptions of slow fluctuations (nominally <0.1 Hz) in neuronal membrane polarization—so-called up and down states—are intriguing (4, 10). Not only does their temporal frequency correspond to that of the spontaneous fluctuations in the fMRI BOLD signal, but their functional consequences may be relevant to an understanding of the variability in task-evoked brain activity as well as behavioral variability in human performance.

William James presciently suggested in 1890 (11) that "Enough has now been said to prove the general law of perception, which is this, that whilst part of what we perceive comes through our senses from the object before us, another part (and it may be the larger part) always comes (in Lazarus's phrase) out of our own head." The brain's energy consumption tells us that the brain is never at rest. The challenge of neuroscience is to understand the functions associated with this energy consumption.

ATMOSPHERE

How Fast Are the Ice Sheets Melting?

Anny Cazenave

Remote-sensing data suggest that ice sheets currently contribute little to sea-level rise. However, dynamical instabilities in response to climate warming may cause faster ice-mass loss.

If the ice sheets covering Greenland and Antarctica were to melt completely, they would raise sea level by about 65 m. But even a small loss of ice mass from the ice sheets would have a great impact on sea level, particularly on low-lying islands and coastal regions. New satellite observations, including those reported by Luthcke *et al.* on page 1286 of this issue (1), now allow estimates of the mass balances of the ice sheets and their evolution through time.

For the past 3000 years, global sea level has remained stable, but since the end of the 19th century, tide gauges have detected global sea-level rises [~ 1.8 mm/year on average over the past 50 years (2, 3)]. Satellite altimetry data document a rate of ~ 3 mm/year since 1993 (4). However, it remains unclear whether the recent rate increase reflects an accelera-

References

1. R. Llinas, *I of the Vortex: From Neurons to Self* (MIT Press, Cambridge, MA, 2001).
2. M. E. Raichle, M. Mintun, *Annu. Rev. Neurosci.* **29**, 449 (2006).
3. A. Peters, B. R. Payne, J. Budd, *Cereb. Cortex* **4**, 215 (1994).
4. B. Haider, A. Duque, A. R. Hasenstaub, D. A. McCormick, *J. Neurosci.* **26**, 4535 (2006).
5. B. A. Olshausen, in *The Visual Neurosciences*, L. M. Chalupa, J. S. Werner, Eds. (MIT Press, Cambridge, MA, 2003), pp. 1603–1615.
6. D. H. Ingvar, *Hum. Neurobiol.* **4**, 127 (1985).
7. D. Gilbert, *Stumbling on Happiness* (Knopf, New York, 2006).
8. J. Hawkins, S. Blakeslee, *On Intelligence* (Holt, New York, 2004).
9. D. A. Leopold, Y. Murayama, N. K. Logothetis, *Cereb. Cortex* **13**, 422 (2003).
10. C. C. H. Petersen, T. T. G. Hahn, M. Mehta, A. Grinvald, B. Sakmann, *Proc. Natl. Acad. Sci. U.S.A.* **100**, 13638 (2003).
11. W. James, *Principles of Psychology* (Henry Holt & Company, New York, 1890), vol. 2, p. 103.
12. M. D. Fox *et al.*, *Proc. Natl. Acad. Sci. U.S.A.* **102**, 9673 (2005).

10.1126/science.1134405

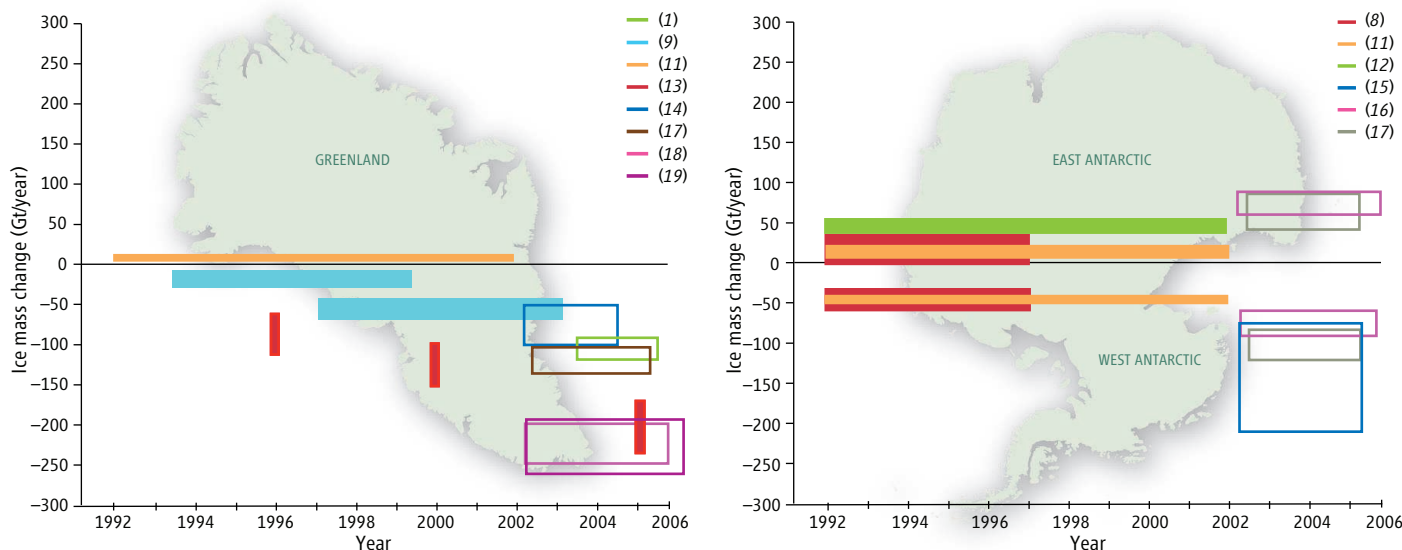
Enhanced online at
www.sciencemag.org/cgi/
content/full/314/5803/1250

tion in sea-level rise or a natural fluctuation on a decadal time scale.

Present-day sea-level rise has several causes. During the past decade, ocean warming has contributed roughly half of the observed rate of sea-level rise (5), leaving the other half for ocean-mass increase caused by water exchange with continents, glaciers, and ice sheets (6). The contribution of mountain glaciers and small ice caps to sea-level rise in the past decade is estimated to be ~ 0.8 mm/year (7). These figures constrain the contribution from ice sheets to less than 1 mm/year in the past decade.

Since the early 1990s, remote-sensing data based on airborne laser and satellite radar altimetry, as well as the space-borne Synthetic Aperture Radar Interferometry (InSAR) technique, have provided the first observations of ice sheet mass balance (8–13). These observations indicate accelerated ice-mass loss in recent years in the coastal regions of southern Greenland. In contrast, slight mass gain is reported in central high-elevation regions. Over Antarctica, remote sensing indicates

The author is at the Observatoire Midi-Pyrenees, 31400 Toulouse, France. E-mail: anny.cazenave@cnes.fr



Ice-sheet mass change estimated by different remote-sensing techniques. (Left) Greenland. (Right) West and East Antarctica. The ice sheet mass change is given in gigatons per year. The numbers refer to different investigations as quoted in

the reference list. Open bars correspond to GRACE results, filled bars to results from other techniques. The estimate from (15) is an average over the whole of Antarctica. On the right, positive values are for East Antarctica and negative values for West.

accelerated mass loss in the western part of the continent (10), whereas the eastern part is gaining some mass as a result of increased precipitation (11, 12).

Because of these contrasting behaviors—mass loss in coastal regions and mass gain in elevated central regions—ice-sheet mass loss exceeds mass gain only slightly. Thus, according to the recent mass-balance estimates, the ice sheets presently contribute little to sea-level rise. However, great uncertainty remains, mainly because of incomplete coverage by remote-sensing surveys, spatial and temporal undersampling, measurement errors, and perturbation from unrelated signals. In addition, each technique has its biases. For example, radar altimetry misses narrow coastal glaciers because of inadequate ground resolution, and ice elevations measured by the radar are much less reliable over steep, undulated surfaces than over flat high-elevation surfaces. Another uncertainty arises because conversion of elevation change to mass change requires assumptions about the surface density of snow or ice to be made.

Since 2002, the NASA/DLR Gravity Recovery and Climate Experiment (GRACE) satellite mission has provided a new tool for precise measurements of ice-sheet mass balance, with nearly complete coverage of the high-latitude regions up to 89°N/S. GRACE measures the spatiotemporal change of Earth's gravity field. Over the ice sheets, this change can be converted into ice-mass change, assuming that the gravity change results from a change in surface mass.

Several studies have reported estimates of Greenland and Antarctica ice-mass change from GRACE (14–19). The GRACE results

confirm those from other remote-sensing techniques, that is, net ice-mass loss from Greenland and West Antarctica and a slight ice-mass gain over East Antarctica (see the figure). The GRACE results over Greenland also suggest accelerated ice-mass loss since 2002, in agreement with InSAR results (13).

However, the GRACE-based mass-balance estimates are highly scattered (see the figure). One reason is the short time span of the analyses (2 to 4 years, depending on the study). Over Greenland, ice mass varies widely from year to year. Because the analyses do not overlap exactly in time, different trend estimates are to be expected.

Another cause of scatter is contamination from geodynamic processes related to Earth's response to ice melt from the last deglaciation. This effect, which depends on poorly known parameters, is mainly available from modeling, with important differences between models. Moreover, over Antarctica, this effect is of the same order of magnitude as present-day ice-mass change.

A third source of uncertainty is the coarse resolution (400 to 600 km) of most GRACE results (14–19). As a result, the estimated ice-sheet mass change includes contributions not only from small isolated glaciers in the vicinity of the ice sheets, but also from other gravity signals (of oceanic, hydrologic, and tidal origin) from surrounding regions. These perturbing signals are still poorly known, and therefore difficult to be corrected for.

To improve the GRACE resolution, Luthcke *et al.* have applied a new approach over Greenland: They determined mass concentrations at a local scale from appropriate processing of the GRACE observations. This

approach differs from the standard method, in which global solutions of the time-varying gravity field are computed, and a regional filter is then applied to extract the mass signal over the area of interest. The new approach minimizes the contamination from signals unrelated to the ice-sheet mass balance and provides results of finer resolution.

Luthcke *et al.* computed ice-mass change in six drainage basins of the Greenland ice sheet, ranging from coastal low-elevation to central elevated regions. They find ice-mass increase in high-elevation regions of northern Greenland, as suggested by satellite altimetry (11), and ice depletion at the margins of southern Greenland, in agreement with InSAR-based glacier discharge estimates (13). The results confirm accelerated ice flow in coastal regions of southeast Greenland. However, the trend is smaller than reported by some other recent GRACE-based studies (18, 19). Over the 2-year period of investigation, Luthcke *et al.*'s estimate of Greenland's contribution to sea-level rise amounts to ~0.3 mm/year.

However, further research is needed to improve estimates of Greenland and Antarctica mass balance (see the figure) and their contribution to sea level. Besides extending the time series of observations and reducing internal errors, it is important to reconcile estimates from different techniques and to eventually use them in synergy.

The greatest uncertainty in sea-level projections is the future behavior of the ice sheets. In recent years, the velocities of outlet glaciers in coastal regions of Greenland and Antarctica have accelerated, showing that a large fraction of ice-mass loss occurs through dynamical processes

rather than surface melting (9, 10, 13). The dynamical response of the ice sheets to present-day climate forcing may thus play a much larger role than previously assumed. Future dynamical instabilities of the ice sheets is of major concern, given their potential impact on sea level (20), yet comprehensive modeling of such dynamical effects is in its infancy.

Improved mass-balance estimates from remote-sensing observations, such as those reported by Luthcke *et al.*, will inform on the ongoing behavior of the ice sheets and help to validate models. This goal requires long time series of satellite observations,

and hence continuity of space missions.

References

1. S. B. Luthcke *et al.*, *Science* **314**, 1286 (2006); published online 19 October 2006 (10.1126/science.1130776).
2. J. A. Church *et al.*, *J. Climate* **17**, 2609 (2004).
3. S. Holgate, P. Woodworth, *Geophys. Res. Lett.* **31**, L07305 (2004).
4. A. Cazenave, R. S. Nerem, *Rev. Geophys.* **42**, RG3001 (2004).
5. S. Levitus, J. I. Antonov, T. P. Boyer, *Geophys. Res. Lett.* **32**, L02604, (2005).
6. A. Lombard *et al.*, *Ocean Dyn.*, in press.
7. M. Dyrgerov, M. F. Meier, INSTAAR, Univ. of Colorado, Boulder, CO, 2005; available at http://instaar.colorado.edu/other/occ_papers.html.
8. E. Rignot, R. Thomas, *Science* **297**, 1502 (2002).
9. W. Krabill *et al.*, *Geophys. Res. Lett.* **31**, L24402 (2004).
10. R. Thomas *et al.*, *Science* **306**, 255 (2004).
11. H. J. Zwally *et al.*, *J. Glaciol.* **51**, 509 (2005).
12. C. H. Davis *et al.*, *Science* **308**, 1898 (2005).
13. E. Rignot, P. Kanagaratnam, *Science* **311**, 986 (2006).
14. I. Velicogna, J. M. Wahr, *Geophys. Res. Lett.* **32**, L18505 (2005).
15. I. Velicogna, J. M. Wahr, *Science* **311**, 1754 (2006).
16. J. L. Chen, C. R. Wilson, D. D. Blankenship, B. D. Tapley, *Geophys. Res. Lett.* **33**, L11502 (2006).
17. G. Ramillien *et al.*, *Global Planet. Change*, in press.
18. J. L. Chen, C. R. Wilson, B. D. Tapley, *Science* **313**, 1958 (2006).
19. I. Velicogna, J. M. Wahr, *Nature* **443**, 329 (2006).
20. R. B. Alley *et al.*, *Science* **310**, 456 (2006).

Published online 19 October 2006;
10.1126/science.1133325
Include this information when citing this paper.

PLANT SCIENCE

Distributing Nutrition

Jonathan D. Gitlin

Hunger claims the lives of 20,000 children a day. Worldwide, one of every three children is underweight and malnourished (1). Eradication of malnutrition and associated childhood mortality is a major mission of the United Nations Millennium Development Goals and will require a shared vision of conservation as well as improvements in agriculture that include increasing the nutritional value of staple crops (2). Advances in basic plant sciences applied to agriculture will be critical for success (3). Strong endorsement of this idea comes from two studies on pages 1295 and 1298 of this issue that provide insight into the mechanisms of nutrient distribution in plants (4, 5). This work reminds us that any effort to enrich the nutritional content of plants requires knowledge of the mechanisms of acquisition and distribution of these nutrients throughout the component parts of the crops that are the dietary staple.

Kim *et al.* (4) combine mutational analysis and imaging to demonstrate an essential role for iron in seedling development—specifically, iron localized to an intracellular compartment called the vacuole in the model plant *Arabidopsis thaliana*. Although abundant, iron is relatively insoluble, and the challenge for all organisms is to acquire adequate amounts while avoiding toxicity (6). Iron is essential for oxygen transport throughout an organism and for cellular (mitochondrial) res-



Dietary crops. A market, or *tianguis*, in Huauchinango, Mexico, with indigenous Mexicans and typical crop-based diets.

piration. Iron deficiency is common, affecting 500 million children in populations with crop-based diets. Infants are at greatest risk because brain growth can quickly outpace dietary availability, resulting in long-term neurocognitive impairment (7). Understanding iron homeostasis in plants is therefore essential to any effort intended to increase the iron content of staple foods as an approach to preventing iron deficiency.

In most organisms, iron that is stored in cells is bound to ferritin, a cytoplasmic protein. Unlike humans, but similar to yeast, plant cells contain vacuoles that function as reservoirs for ions and metabolites and could also serve as sites of iron storage (8). Kim *et al.* identify VIT1 as the *Arabidopsis* ortholog of a vacuolar iron transporter, CCC1, previously

New insights into how plants store and mobilize nutrients, such as iron, can help in the fight against world hunger.

identified in yeast. They show that this protein rescues the iron-sensitive phenotype of a yeast mutant that lacks CCC1, mediates iron sequestration into yeast vacuoles, and is highly expressed in developing seeds—an important food source worldwide. However, there is no difference in the total iron content of seeds or shoots between wild-type *Arabidopsis* plants and mutant plants that lack the gene encoding VIT1 (*vit1*). So is VIT1 required for plant iron homeostasis?

In an imaging tour de force, Kim *et al.* use x-ray fluorescence microtomography to demonstrate a dramatic loss of iron in germinating seeds that lack VIT1, specifically in provascular cells of the hypocotyl, radicle, and cotyledon embryonic seed tissues. This finding implicates the vacuole of provascular cells as critical to iron storage in wild-type seeds. Consistent with this idea, *vit1* seedlings germinate poorly under conditions that limit iron availability from the soil. These findings highlight the need to understand nutrient distribution in assessing homeostasis, as well as the importance of noninvasive, three-dimensional quantitative element analysis in living samples. Such approaches will find broad application to issues of nutrient homeostasis in living organisms.

In a related study, Uauy *et al.* (5) characterize *Gpc-B1* from wild emmer wheat as a simple Mendelian quantitative trait locus (genomic DNA that is associated with a particular trait that varies continuously across a population) that is associated with accelerated senescence and increases in grain zinc, iron, and protein content. This wheat is ancestral to

The author is in the Department of Pediatrics, Washington University School of Medicine, St. Louis, MO 63110, USA. E-mail: gitlin@kids.wustl.edu

chronosequences (7) or soil respiration measurements (31). The assumption that soils are in a steady state is also called into question, especially because it is recognized that refractory OC has been building up in soils exposed since the last glacial (1, 5). This new paradigm likely has its main impact on carbon budget models that calculate sources, sinks, and fluxes within the global carbon cycle on longer time scales (>1000 years). This could be of relevance, for example, to studies that link vegetation type to soil carbon content in order to estimate changing carbon storage on land through time (9). It places the terrestrial biosphere in a more prominent position as a slow but progressively important atmospheric carbon sink on geologic time scales and may even influence current predictions about carbon cycling and soil carbon storage in response to elevated atmospheric CO₂ levels.

References and Notes

- R. Amundson, *Annu. Rev. Earth Planet. Sci.* **29**, 535 (2001).
- J. I. Hedges, R. G. Keil, *Mar. Chem.* **49**, 81 (1995).
- E. A. Davidson, I. A. Janssens, *Nature* **440**, 165 (2006).
- P. D. Falloon, P. Smith, *Biol. Fertil. Soils* **30**, 388 (2000).
- J. W. Harden, E. T. Sundquist, R. F. Stallard, R. K. Mark, *Science* **258**, 1921 (1992).
- E. A. Paul, H. P. Collins, S. W. Leavitt, *Geoderma* **104**, 239 (2001).
- W. H. Schlesinger, *Nature* **348**, 232 (1990).
- M. S. Torn et al., *Nature* **389**, 170 (1997).
- J. M. Adams, H. A. Faure, *Global Planet. Change* **16-17**, 3 (1998).
- B. D. Bornhold et al., *Proceedings of the Ocean Drilling Program, Initial Reports, 1695* (Ocean Drilling Program, College Station, TX, 1998), pp. 5–138.
- S. M. Gucluer, M. G. Gross, *Limn. Oceanogr.* **9**, 359 (1964).
- M. R. McQuoid, M. J. Whitticar, S. E. Elvert, T. F. Pederson, *Mar. Geol.* **174**, 273 (2001).
- A. J. Nederbragt, J. W. Thurow, *Mar. Geol.* **174**, 95 (2001).
- Materials and methods are available as supporting material on Science Online.
- J. W. Collister, G. Rieley, B. Stern, G. Eglinton, B. Fry, *Org. Geochem.* **21**, 619 (1994).
- M. B. Yunker, R. W. MacDonald, *Org. Geochem.* **34**, 1429 (2003).
- F. S. Brown, M. J. Baedecker, A. Nissenbaum, I. R. Kaplan, *Geochim. Cosmochim. Acta* **36**, 1185 (1972).
- M.-Y. Sun, S. G. Wakeham, *Geochim. Cosmochim. Acta* **58**, 3395 (1994).
- F. G. Prahl, G. J. De Lange, S. Scholten, G. L. Cowie, *Org. Geochem.* **27**, 141 (1997).
- Y. Huang, *Soil Sci. Soc. Am. J.* **63**, 1181 (1999).
- M. J. Kennedy, D. R. Pevear, R. J. Hill, *Science* **295**, 657 (2002).
- L. M. Mayer, L. L. Schick, K. R. Hardy, R. Wagai, J. McCarthy, *Geochim. Cosmochim. Acta* **68**, 3863 (2004).
- M. Church, O. Slaymaker, *Nature* **337**, 452 (1989).
- P. McLaren, T. Tuominen, in *Health of the Fraser River Aquatic Ecosystem, a Synthesis of Research Conducted under the Fraser River Action Plan, DOE FRAP 1998-11*, C. Colin, T. Tuominen, Eds. (Environment Canada, Vancouver, BC, Canada, 1999), vol. 1, chap. 3.4.
- M. H. Conte, J. C. Weber, *Global Biogeochem. Cycles* **16**, 10.1029/2002GB001922 (2002).
- R. H. Smittenberg et al., *Paleoceanography* **19**, 10.1029/2003PA000927 (2004).
- D. J. Kovanen, D. J. Easterbrook, *Quat. Res.* **57**, 208 (2002).
- J. W. Collister, É. Lichtfouse, G. Hieshima, J. M. Hayes, *Org. Geochem.* **21**, 645 (1994).
- G. Gleixner, et al., *Org. Geochem.* **33**, 357 (2002).
- E. Lichtfouse et al., *Geochim. Cosmochim. Acta* **61**, 1891 (1997).
- S. Trumbore, *Ecol. Appl.* **10**, 339 (2000).
- We thank the staff at the National Ocean Sciences Accelerator Mass Spectrometry Facility at Woods Hole, MA, USA, for help during preparation for ¹⁴C analysis; M. Baas, M. Kienhuis (Royal Netherland Institute of Sea Research), and D. Montluçon (Woods Hole Oceanographic Institution) for assistance with the *n*-alkane isolation; The Ocean Drilling Project for providing subsamples obtained at leg 1695; and M. J. Whitticar (University of Victoria, Canada), for providing the pre- and post-bomb sediments. This research was primarily conducted by R.H.S., supported by a grant to J.S.S.D. from the Research Council for Earth and Life Science (ALW) with financial support from the Netherlands Organization for Scientific Research (NWO), and a grant to T.I.E. from NSF (OCE-0137005).

Supporting Online Material

www.sciencemag.org/cgi/content/full/314/5803/1283/DC1

Materials and Methods

Fig. S1

Table S1

References

1 May 2006; accepted 10 October 2006

10.1126/science.1129376

Recent Greenland Ice Mass Loss by Drainage System from Satellite Gravity Observations

S. B. Luthcke,^{1*} H. J. Zwally,² W. Abdalati,² D. D. Rowlands,¹ R. D. Ray,¹ R. S. Nerem,³ F. G. Lemoine,¹ J. J. McCarthy,⁴ D. S. Chinn⁴

Mass changes of the Greenland Ice Sheet resolved by drainage system regions were derived from a local mass concentration analysis of NASA–Deutsches Zentrum für Luft- und Raumfahrt Gravity Recovery and Climate Experiment (GRACE mission) observations. From 2003 to 2005, the ice sheet lost 101 ± 16 gigaton/year, with a gain of 54 gigaton/year above 2000 meters and a loss of 155 gigaton/year at lower elevations. The lower elevations show a large seasonal cycle, with mass losses during summer melting followed by gains from fall through spring. The overall rate of loss reflects a considerable change in trend (–113 ± 17 gigaton/year) from a near balance during the 1990s but is smaller than some other recent estimates.

Mass changes in the Greenland Ice Sheet are of considerable interest because of its sensitivity to climate change and the potential for an increasing contribution of Greenland ice loss to rising sea level. Observations and models have shown that in recent years Greenland has experienced increased melt (1), thinning at the margins (2–4), and increased discharge from many outlet glaciers (5). At the same time, the ice sheet has been growing in its interior (3, 4, 6).

These recent changes in the Greenland Ice Sheet and the wide range of mass-balance estimates (7) highlight the importance of methods for directly observing variations in ice sheet

mass. Moreover, the fact that some regions are shedding mass dramatically, whereas others are not (2–5), indicates a clear need for measurements with a spatial resolution that allows assessment of the behavior of individual drainage systems (DSs). The local mass concentration analysis presented here provides an assessment of mass balance of individual Greenland DS regions, subdivided by elevation, as well as the overall ice sheet mass balance.

Direct measurements of mass change have been enabled by the NASA–Deutsches Zentrum für Luft- und Raumfahrt Gravity Recovery and Climate Experiment (GRACE) mission (8). Since its launch in March 2002, GRACE has

been acquiring ultra-precise (0.1 μm/s) intersatellite K-band range and range rate (KBRR) measurements taken between two satellites in polar orbit about 200 km apart. The changes in range rate sensed between these satellites provide a direct mapping of static and time-variable gravity.

Recent GRACE-based mass balance estimates of Antarctica (9) and Greenland (10, 11) have been derived from the monthly spherical-harmonic gravity fields produced by the GRACE project. Although these solutions represent an important advance in the use of gravity measurements to assess ice sheet mass balance, they are limited in their temporal and spatial resolution. For example, the recent results presented in (11) showed sizable mass loss spread over the entire Greenland continent, in contrast with recent studies that indicated loss concentrated on the margins (2–5) and growth in the interior (3, 4, 6). In addition, the fundamental measurements being made by GRACE contain far more information than is currently being exploited by techniques that rely on these monthly

¹Planetary Geodynamics Laboratory, Code 698, NASA Goddard Space Flight Center, Greenbelt, MD 20771, USA. ²Cryospheric Sciences Branch, Code 614.1, NASA Goddard Space Flight Center, Greenbelt, MD 20771, USA.

³Colorado Center for Astrodynamics Research, Cooperative Institute for Research in Environmental Sciences, Department of Aerospace Engineering Sciences, University of Colorado, Boulder, CO 80309, USA. ⁴Science Division, SGT Incorporated, Greenbelt, MD 20770, USA.

*To whom correspondence should be addressed. E-mail: Scott.B.Luthcke@nasa.gov

spherical-harmonic fields. Close examination of the KBRR measurements reveals coherent mass variation signals at better-than-400-km full wavelength spatial and 10-day temporal resolution at the mid-latitudes (12) and still better resolution at high latitudes.

Our approach to estimating ice sheet mass changes followed a strategy of preserving the gravity information contained within the GRACE KBRR observations. This was accomplished through an innovative processing of the GRACE intersatellite range-rate measurements (13) and the parameterization of local mass variations as mass concentrations (mascons). Mascons were estimated from short arc solutions of GRACE KBRR data exclusively within a local area of interest (12). The regional solution exploits the fact that the signal from a mass concentration observed in the GRACE KBRR data is centered over the mass concentration and is spatially limited in extent. The mathematical formulation of mascon parameters, the details of the local mascon approach, and the results of a simulation that validate the method are provided in (14). The results of the simulations show that the mascon approach is capable of recovering the spatial distribution and magnitude of realistic and complex ice mass change signal to better than 90% (14).

For our ice sheet analysis, a mascon parameter corresponds to a surplus or deficit of mass in an irregularly shaped DS region (Fig. 1) defined by surface slopes and climatology (15) and subdivided into surface elevation above and below 2000 m. Exterior regions (as outlined in Fig. 1) as well as daily baseline state parameters were estimated to account for mass variations occurring outside our Greenland DS regions of interest (14). The mascon estimates are relative to models of both static and time varying gravity effects (e.g., tides and atmospheric mass redistribution) in order to isolate ice mass change (14).

We derived mascon solutions from GRACE KBRR data for each DS region (Fig. 1) every 10 days from July 2003 through July 2005 (Table 1). The individual elevation-dependent mascon solution time series can be summed over each 10-day interval to produce time series for the six overall DSs (Fig. 2) and time series for regions above and below 2000 m elevation (Fig. 3). The results (Table 1 and Figs. 2 and 3) represent the total observed mass variation, including the trends from glacial isostatic adjustment (GIA). Included separately in Table 1 is the computed GIA trend from ICE-5G using a 90-km lithosphere and VM2 viscosity model (16).

The northern DSs 1 and 2 and the southwest DS 5 are nearly in mass balance (Fig. 2), considering the associated error bars and the GIA noted in Table 1. DSs 3, 4, and 6 all exhibit significant mass loss, with DS 4, the southeast, dominating the overall mass loss. Figure 3 presents our mascon time series for the regions above and below 2000-m elevation. For the 2 years (July 2003 to July 2005), our solutions

(Fig. 3) show a moderate growth of 54 ± 12 Gton/year for the high-elevation Greenland interior, with a significant loss of 155 ± 26 Gton/year occurring in the low-elevation coastal regions. Therefore, we obtain a total Greenland trend of -101 ± 16 Gton/year. These trends have been corrected for GIA and scaled by 1.1 to account for potential signal loss as determined in the simulation analysis (14). Treatment of the associated errors is discussed in (14). The mass loss is dominated by loss in the eastern low-elevation coastal regions and the southeast DS 4. Our overall Greenland mass trend of -101 ± 16 Gton/year is consistent with the GRACE-based analysis by (17), which determined a trend of -118 ± 14 Gton/year for the time period of July 2002 to March 2005. However, these overall trends are nearly a factor of 2 smaller than the recent GRACE-based trend determined in (11). The results presented in (11) show significant

mass loss over the entire continent and therefore are difficult to reconcile with known mass loss concentrated in the low-elevation coastal regions and gain in the interior.

The high-elevation interior region solutions show little annual cycle, with an overall amplitude of 13 ± 9 Gton, whereas in contrast the low-elevation coastal region solutions resolve a significant annual cycle with an amplitude of 150 ± 27 Gton (Table 1 and Fig. 3). The annual cycle of the low-elevation coastal region exhibits significant mass shedding beginning in May-June and ending in October, corresponding to summer melt (Fig. 3). The largest annual cycle is found in the southwest DS 5. A nearly semiannual signal most noticeable in DS 2 is an artifact caused by mismodeled ocean tides (14).

The temporal and spatial resolution of the GRACE mascon solutions provides important insights into the ice sheet behavior and the

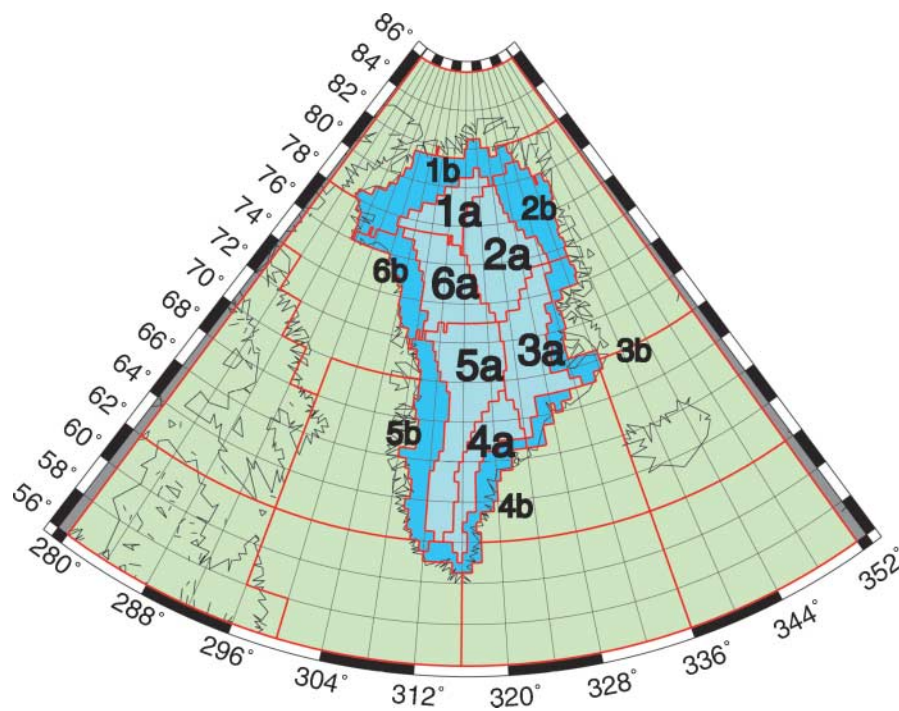


Fig. 1. Greenland DS mascon regions: regions above 2000 m elevation are labeled "a," and those below are labeled "b." Exterior region mascons outside of Greenland are also shown outlined in red.

Table 1. Summary of Greenland drainage system mascon solutions above and below 2000-m elevation (July 2003 to July 2005). GIA calculated from ICE-5G with use of a 90-km lithosphere and VM2 viscosity model (16).

Drainage system	Observed mass change (Gton/year)		GIA (Gton/year)		Annual amplitude (Gton)	
	>2000 m	<2000 m	>2000 m	<2000 m	>2000 m	<2000 m
1	13 ± 2	-4 ± 4	0	2	7 ± 2	34 ± 5
2	40 ± 2	-32 ± 2	-1	2	12 ± 2	11 ± 3
3	50 ± 3	-75 ± 2	-1	0	8 ± 4	24 ± 2
4	-38 ± 11	-33 ± 3	-1	0	12 ± 13	33 ± 3
5	3 ± 3	-3 ± 13	-4	-3	19 ± 3	62 ± 14
6	-27 ± 3	6 ± 5	-1	0	14 ± 3	20 ± 6
Greenland	41 ± 8	-140 ± 24	-8	1	13 ± 9	150 ± 27

quality of the mascon solutions. The moderate growth of the high-elevation interior ice sheet with significant mass shedding of the low-elevation coastal regions is consistent with other recent studies (1–6). In addition, the solutions exhibit a relatively small annual cycle for the high-elevation interior ice sheet, consistent with low temperatures, negligible melting, and small seasonal variation in precipitation. The low elevations show a large annual cycle, with the largest in the southwest DS 5. These results are consistent with warm summer temperatures of the coastal regions in general and, combined with shallow slopes for DS 5 in particular, lead to the most extensive summer melt (18). There-

fore, our mascon time series for the low elevations exhibit seasonal characteristics that are very consistent with the well-known net ablation during summer melt followed by growth during winter, as shown for example by radar altimeter data (3) and surface mass balance models (19).

Comparison of our 2003–2005 ice mass trends by DS in Table 2 to the 1992–2002 trends computed from satellite radar and airborne laser altimetry (3) provides insights into the evolution of the ice sheet. The changes of the trends with time of the two most northerly DSs, 1 and 2, are not significantly different from zero, which is consistent with the lack of glacier acceleration

(5) or detected icequakes (20) reported for those areas. DS 3 in the east appears to have changed by –20 Gton/year from a slightly negative balance (–5 Gton/year) to a significantly negative overall balance of –25 Gton/year, with very large mass shedding in the low-elevation coastal region and growth at high elevations (Table 1). Although DS 3 had one accelerating glacier (5) and icequakes in two glaciers (20), it has also had a large average annual mass input of 42 Gton/year (3) and is therefore very sensitive to interannual variations or trends in precipitation and ice accumulation. Our largest observed change (–61 Gton/year) occurred in DS 4 in the southeast, whereas the other significant negative change occurred in DS 6 in the west (–32 Gton/year), consistent with glacier accelerations (5) and increases in icequakes (20) in that system. In particular, the acceleration of three glaciers in DS 4 indicated an increase in the rate of loss in 2005, compared with that in 1996, of –56 Gton/year (5), which is comparable to our change of –61 Gton/year. In DSs 5 and 6, the change from glacier accelerations was –25 Gton/year (5), which compares well with our total change of –37 Gton/year that includes changes in surface balance as well as changes in glacier discharge. Although the extent to which meaningful conclusions can be drawn from a 2-year time series is limited because of the influence of interannual variations, the consistency of our results with all other indications of accelerating mass loss (1, 4, 5, 19) strongly supports our interpretation that a significant change in the Greenland mass balance has occurred primarily in DSs 3, 4, and 6.

The high temporal resolution of the mascon solutions provides unprecedented observation of mass change events and provides the opportunity to apply filtering techniques to reduce the solution noise. By reliably resolving ice mass change observations into ice sheet DS scales subdivided by surface elevation, the mascon solutions provide the ability to separate the areas of rapid loss [e.g., the southeast DS 4 and the low-elevation coastal regions (Figs. 2 and 3)] from areas of slower loss or even gain (e.g., high-elevation interior regions). The mascon solutions provide a better basis for comparison to passive microwave-derived melt data (18) and surface mass balance models (19) and facilitate the comparison to flux-based methods (5) and altimetric methods (2–4, 6, 21) that examine individual drainage basins.

Our GRACE mascon solutions provide a direct measure of mass changes on the scale of DSs subdivided into regions above and below 2000-m surface elevation. In contrast with other recent gravity-based mass balance estimates (10, 11, 17), our mascon solutions exhibit improved spatial resolution, delineating high-elevation interior region growth and substantial mass loss for the low-elevation coastal regions. In addition, the mascon solutions show improved temporal resolution, delineating the large season-

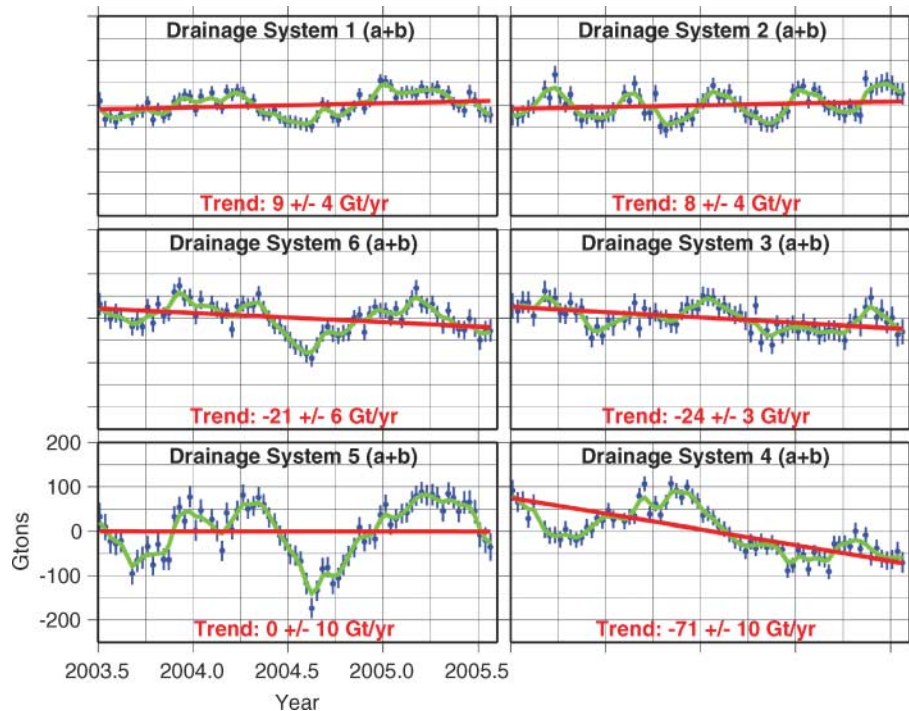


Fig. 2. Greenland drainage systems 2-year (July 2003 to July 2005) mascon time series (summing regions above and below 2000-m elevation for each system) derived from GRACE KBRR data: 10-day estimates (blue dots with error bars); Gaussian 1-day filter with 30-day window applied to 10-day estimates (green line); and trend (red line) recovered from simultaneous estimation of bias, trend, annual and semi-annual sinusoid. Trends have not been corrected for GIA. Error bars indicate 1- σ calibrated uncertainties. Gt/yr, Gton/year.

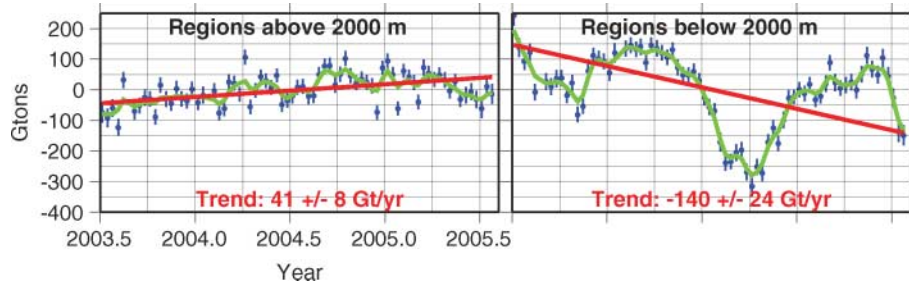


Fig. 3. Time series computed from the sum of mascon region solutions above and below 2000-m elevation: 10-day estimates (blue dots with error bars); Gaussian 1-day filter with 30-day window applied to 10-day estimates (green line); and trend (red line) recovered from simultaneous estimation of bias, trend, annual and semi-annual sinusoid. Trends have not been corrected for GIA. Error bars indicate 1- σ calibrated uncertainties.

Table 2. Comparison of mascon-derived trends with previous values determined from satellite and airborne altimetry (3). The mascon-derived trends were corrected for GIA and potential signal loss (~9%) as determined from simulation analysis (14). Errors computed as in (14) along with assuming 100% error in GIA.

Drainage system	2003–2005 mascon-derived ice mass trend (Gton/year)	1992–2002 altimeter-derived ice mass trend (3) (Gton/year)	Delta (2003–2005) – (1992–2002) (Gton/year)
1	8 ± 5	1.6 ± 0.3	6 ± 5
2	8 ± 4	8.8 ± 0.2	-1 ± 4
3	-25 ± 4	-4.9 ± 2.0	-20 ± 4
4	-77 ± 11	-15.7 ± 1.2	-61 ± 11
5	7 ± 13	11.4 ± 0.8	-5 ± 13
6	-22 ± 7	10.5 ± 0.5	-32 ± 7
Greenland	-101 ± 16	11.7 ± 2.5	-113 ± 17

al cycle for the low-elevation coastal regions and observing the summer melt and winter growth cycles. Our finding of an overall mass loss of 101 ± 16 Gton/year for 2003 to 2005 is consistent with the finding of near balance during the 1990s (3) and with the recent results on increased melt rates (1), acceleration of outlet glaciers (5, 20), and the increasingly negative surface balance in recent years (22). The Greenland mass loss contributes 0.28 ± 0.04 mm/year to global sea level rise, which is nearly 10% of the 3 mm/year rate recently observed by satellite altimeters (23). The observed change from the 1990s of -113 ± 17 Gton/year represents a change from a small growth of about 2% of the annual mass input to a loss of about 20%, which is a significant change over a period of less than 10 years (24). This result is in very good agreement with the change in trend of -117 Gton/year from 1996 to 2005 determined from radar interferometry (5). During the 1990s, the observed thinning at the margins and the growth inland were both expected responses to climate warming. Our new results suggest that the processes of significant ice depletion at the margins, through melting and glacier acceleration, are beginning to dominate the interior growth as climate warming has continued.

References and Notes

1. An update of (18) posted at <http://cires.colorado.edu/science/groups/steffen/greenland/melt2005> shows a 31% increase in mean melt area between 1979 and 2005.
2. W. Krabill *et al.*, *Geophys. Res. Lett.* **31**, L24402 (2004).
3. H. J. Zwally *et al.*, *J. Glaciol.* **51**, 509 (2005).
4. R. Thomas *et al.*, *Geophys. Res. Lett.* **33**, L10503 (2006).
5. E. Rignot, P. Kanagaratnam, *Science* **311**, 986 (2006).
6. O. M. Johannessen, K. Khvorostovsky, M. W. Miles, L. P. Bobylev, *Science* **310**, 1013 (2005); published online 20 October 2005 (10.1126/science.1115356).
7. For mass balance within the 1992–2002 time period, the following estimates have been published: $+11 \pm 3$ Gton/year for 1992–2002 (3), -46 Gton/year for 1993/4 – 1998/9 (21), -72 ± 11 Gton/year for 1997–2003 (2), and -83 ± 29 and -127 ± 29 Gton/year for 1996 and 2000, respectively (5). If the correction for firn compaction used in the radar altimeter analysis (3) is applied to the airborne altimeter estimates (2, 4, 21), the difference between the two approaches is reduced by about 23 Gton/year, as reflected by revised airborne values of -4 to -50 Gton/year for 1993 to 1999 (4).

8. B. D. Tapley, S. Bettadpur, J. C. Ries, P. F. Thompson, M. M. Watkins, *Science* **305**, 503 (2004).
9. I. Velicogna, J. Wahr, *Science* **311**, 1754 (2006); published online 1 March 2006 (10.1126/science.1123785).
10. I. Velicogna, J. Wahr, *Geophys. Res. Lett.* **32**, L18505 (2005).
11. J. L. Chen, C. R. Wilson, B. D. Tapley, *Science* **313**, 1958 (2006); published online 10 August 2006 (10.1126/science.1129007).
12. D. Rowlands *et al.*, *Geophys. Res. Lett.* **32**, L04310 (2005).
13. S. B. Luthcke *et al.*, *Geophys. Res. Lett.* **33**, L02402 (2006).
14. Materials and methods are available as supporting material on Science Online.
15. H. J. Zwally, M. B. Giovinetto, *Ann. Glaciol.* **31**, 126 (2000).
16. W. R. Peltier, *Annu. Rev. Earth Planet. Sci.* **32**, 111 (2004).

17. G. Ramillien *et al.*, *J. Global Planet. Change* **53**, 10.1016/j.jgloplacha.2006.06.003 (2006).
18. W. Abdalati, K. Steffen, *J. Geophys. Res.* **106**, 33983 (2001).
19. J. E. Box *et al.*, *J. Clim.* **19**, 2783 (2006).
20. G. Ekstrom, M. Nettles, V. C. Tsai, *Science* **311**, 1756 (2006).
21. W. Krabill *et al.*, *Science* **289**, 428 (2000).
22. E. Hanna *et al.*, *J. Geophys. Res.* **110**, D13108 (2005).
23. A. Cazenave, R. S. Nerem, *Rev. Geophys.* **42**, 10.1029/2003RG000139 (2004). An update is posted at <http://sealevel.colorado.edu>.
24. For the 1990s, we used the small 11 Gton/year mass gain from (3) and noted that the negative balances discussed in (7) either would give significantly less negative changes than 113 Gton/year or would give positive changes, in contradiction to the evidence for increases in melt and glacier accelerations. Also, our 113 ± 17 Gton/year is in good agreement with the change in mass flux of 117 Gton/year from 1996 to 2005 from radar interferometry (5).
25. We acknowledge NASA's Solid Earth and Natural Hazards Program, NASA's Cryospheric Sciences Program, and NASA's Ice, Cloud, and Land Elevation Satellite and GRACE missions for their support of this research and the quality of the GRACE Level 1B products produced by our colleagues at the Jet Propulsion Laboratory. We thank S. Klosko, T. Williams, and D. Pavlis for their many contributions and the reviewers for their astute commentary.

Supporting Online Material

www.sciencemag.org/cgi/content/full/1130776/DC1
Materials and Methods
Fig. S1

2 June 2006; accepted 10 October 2006

Published online 19 October 2006;

10.1126/science.1130776

Include this information when citing this paper.

Abundance Distributions Imply Elevated Complexity of Post-Paleozoic Marine Ecosystems

Peter J. Wagner,^{1*} Matthew A. Kosnik,² Scott Lidgard¹

Likelihood analyses of 1176 fossil assemblages of marine organisms from Phanerozoic (i.e., Cambrian to Recent) assemblages indicate a shift in typical relative-abundance distributions after the Paleozoic. Ecological theory associated with these abundance distributions implies that complex ecosystems are far more common among Meso-Cenozoic assemblages than among the Paleozoic assemblages that preceded them. This transition coincides not with any major change in the way fossils are preserved or collected but with a shift from communities dominated by sessile epifaunal suspension feeders to communities with elevated diversities of mobile and infaunal taxa. This suggests that the end-Permian extinction permanently altered prevailing marine ecosystem structure and precipitated high levels of ecological complexity and alpha diversity in the Meso-Cenozoic.

Marine ecosystem complexity is thought to have increased over the past 540 million years, in terms both of the alpha [i.e., local (1)] diversity of fossilized assemblages and of the numbers of basic ecological types (i.e., “guilds”) (2–5). Ecological theory predicts that ecosystem complexity affects relative-abundance distributions (RADs) (6). Therefore, if fossiliferous assemblages adequately reflect original communities, then RADs implying interactions and/or a multiplicity of basic ecologies should become more common over time, and

RADs implying simple partitioning and/or limited interaction should become less common. Taphonomic studies show that death assemblages can accurately reflect one aspect of RADs of skeletonized taxa within living communities, namely, rank-order abundance (7). Moreover, paleoecological

¹Department of Geology, Field Museum of Natural History, 1400 South Lake Shore Drive, Chicago, IL 60605, USA.

²School of Marine and Tropical Biology, James Cook University, Townsville, QLD 4811, Australia.

*To whom correspondence should be addressed. E-mail: pwagner@fmnh.org